Relationship Between Lateral Field Excited AT-Cut Quartz Crystal Microbalance Operation and Acoustic Plate Modes

Jequil S. R. Hartz and John F. Vetelino
Frontier Institute for Research in Sensor Technologies
University of Maine, Orono, ME, USA
Email: jequil.hartz@maine.edu, john.vetelino@maine.edu

Nuri W. Emanetoglu
Department of Electrical & Computer Engineering
University of Maine, Orono, ME, USA
Email: nuri.emanetoglu@maine.edu

Abstract— The operational modes of lateral field excited (LFE) quartz crystal microbalances (QCMs) under various electrical boundary conditions have been under investigation for use in sensing applications. The present results indicate connections between the behaviors of acoustic plate modes (APMs) and LFE-QCM modes. The influences of deposited thin conducting and semiconducting films on the mode responses of LFE-QCMs strongly agree with reported effects on APMs. Thus the main operating modes of LFE devices are concluded to be laterally varying APMs, which may be close in character to thickness modes. Mode response changes caused by slowly varying surface curvature are explained from this perspective. The consistency of the usual LFE thickness mode coupling formalism is evaluated, and the superposition of partial waves method is found to be more appropriate for analyzing LFE devices. This view of LFE devices operating through APMs supports improved sensing applications and investigations through access to existing APM knowledge.

Index Terms—lateral field excitation, acoustic plate modes, quartz crystal microbalance, acoustic wave sensor

I. INTRODUCTION

Acoustic wave devices fabricated using thin piezoelectric substrates are common for wireless signal filtering and sensing applications. These devices operate through acoustic waves bound by the device structure and coupled to the electric field. For bulk acoustic wave (BAW) devices like solidly mounted resonators (SMRs) and quartz crystal microbalances (QCMs), the operating modes are standing waves confined by the substrate thickness, referred to as thickness modes [1]. The device may generate laterally propagating acoustic plate waves (APWs) that leak acoustic energy from the main mode or become trapped as spurious acoustic plate modes (APMs) [2]. BAW devices are thus designed to confine the thickness modes strongly in specific substrate regions while minimizing the presence of APWs. Conversely, laterally varying resonators (LVRs) [2] and surface acoustic wave (SAW) devices generally operate through APW solutions, where SAW plates are far thicker than the lateral wavelength.

Thickness field excitation (TFE) [3] and lateral wave excitation (LWE) are the standard approaches to the transduction of acoustic waves in piezoelectric substrates. Thickness field excitation is commonly applied to SMRs and QCMs via electrodes on both major faces of the substrate to induce thickness modes. Lateral wave excitation is a more versatile method where laterally propagating waves are excited by the lateral generation of alternating stresses. Interdigitated

transducers (IDTs) produce a laterally varying electrical wave at a substrate surface and are commonly used for LWE of acoustic waves in LVRs and SAW devices. The bulk thickness and SAW modes are dual cases dependent on orthogonal substrate dimensions. The BAW thickness modes depend on the substrate thickness, and SAWs depend on the lateral acoustic wavelength. Between these limits are APWs that depend on the ratio of substrate thickness to lateral wavelength [1]. However, TFE occurs through an alternating electric field, not a spatially varying thickness electrical wave, and the acoustic wavelength is dependent on the substrate thickness. The lateral counterpart to TFE is excitation via a lateral alternating electric field, referred to as lateral field excitation (LFE). Some works refer to the use of IDTs on a single surface as LFE because the LWE method relies on alternating LFE regions [2]. Another method of LWE uses alternating TFE regions.

The immediate benefit of LFE-based methods is the metallization of a single surface, which reduces fabrication complexity. Recently, laterally excited bulk acoustic resonators (XBARs) [4] operating through an APM have been under consideration for up-and-coming 5G wireless applications due to the inherent mode benefits and tunability. The LFE approach shows similar promise for sensing applications when applied to QCMs [5]. The remaining bare surface of these LFE-QCMs can detect both mechanical and electrical changes in a sensing target, a stark improvement over the mostly mechanical sensing of QCMs excited through TFE. However, the nature of LFE-QCM operation for all likely sensing target measurands is still under investigation. This work aims to disclose the connections between LFE-QCM operation and APMs through new data and existing literature. This relationship has not been made abundantly clear in the current literature and will further current understanding of how LFE modes change under varying electrical boundary conditions.

II. ACOUSTIC PLATE WAVES

Piezoelectric planar waveguides [Fig. 1(a)], with crystal-lographic (X, Y, Z) and rotated plate (x_1, x_2, x_3) coordinate systems, guide APWs that propagate laterally along a direction within the x_1x_2 -plane. These APWs are superpositions of partial (plate) waves [1], which propagate obliquely while reflecting at the $x_3 = \pm \frac{h}{2}$ surfaces, where h is the plate thickness. For infinitely lateral waveguides, the possible APWs

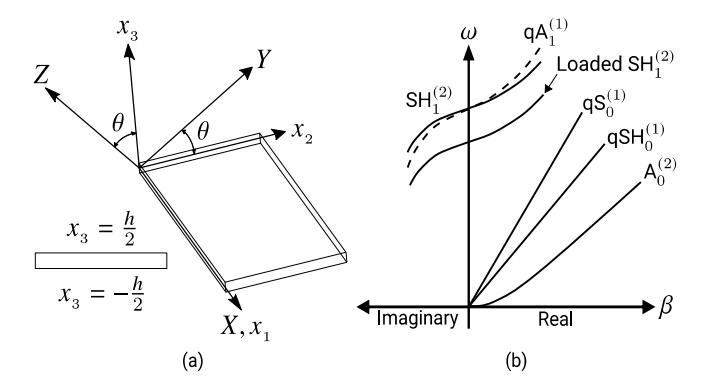


Fig. 1. (a) Piezoelectric acoustic waveguide of thickness h with superposed crystallographic and rotated coordinate systems and (b) portions of AT-cut quartz dispersion branches for frequency ω and lateral wavenumber β .

at their characteristic combinations of frequency ω and lateral wavenumber β are given by dispersion relations. Portions of the usual dispersion branch profiles for AT-cut [$\theta = 54.75^{\circ}$ in Fig. 1(a)] quartz are shown in Fig. 1(b). The trapped APMs depend on the lateral variation of the waveguide, such as laterally varying thickness or loading. Mechanically, the three displacement components are split into two APW families – Lamb and shear horizontal (SH) waves [1]. Lamb waves have elliptical displacement polarization in the sagittal plane spanned by the thickness (x_3) and chosen lateral propagation direction. Shear horizontal waves displace normal to the sagittal plane. Quasi waves [6] may also occur, where the Lamb and SH components are mixed. These waves are delineated by the prefix "q" before the dominant wave type in this work.

Piezoelectrically, there are several coupling cases for Lamb and SH waves with the electrical potential wave. Depending on substrate anisotropy and the lateral propagation direction, the piezoelectric coupling causes stiffened SH, stiffened Lamb, or general waves [7]. Both the Lamb and the SH waves are split into symmetric (S) and antisymmetric (A) groups based on displacement symmetry about the substrate midplane $(x_3 = 0)$. Each of the S and A waves has a dispersion branch [Fig. 1(b)]. Generally, the number of nodal points along the substrate thickness is the wave order. Therefore, higher-order (nonzero-order) APWs may be visualized as laterally propagating thickness modes. Lamb waves are referred to by their symmetry and order, while SH waves are designated by "SH" and their order. For the propagation direction, the axis index is superscripted. For example, $qA_1^{(1)}$ in Fig. 1(b) is the quasi antisymmetric Lamb wave for propagation along x_1 .

Thickness modes occur at the nonzero frequencies where β is zero, the cutoff frequencies. The thickness modes are referred to as pure or quasi based on their polarizations relative to the plate coordinate system [3]. For APWs subject to traction-free $x_3 = \pm \frac{h}{2}$ surfaces, the waves displace at the surfaces. Mechanical surface loading of the APWs causes the dispersion branches to shift [Fig. 1(b)]. For standard AT-cut QCMs, the stiffened SH₁⁽²⁾ branch and corresponding resonance frequencies shift downward. For APWs subject to

electrically open $x_3 = \pm \frac{h}{2}$ surfaces, nonzero surface potential indicates that the coupled APWs are impacted by electrical surface loading, allowing APM sensors to have acoustoelectric interactions [8] with electrical media [5]. As electrical loading also influences the dispersion branches [9], varied surface loading in general causes lateral differences in allowed APWs. Higher-order APWs are then trappable/propagate in specific regions and attenuate outside of them [10]. Mechanical energy trapping allows standard QCMs to be held by their edges while the active sensing region is unperturbed at the center.

III. LATERAL FIELD EXCITATION OF AT-CUT QUARTZ

The application of LFE has been under investigation for AT-cut QCMs due to the temperature-compensated pure slow thickness shear mode (TSM) of AT-cut quartz. These LFE-QCMs are wafer-shaped macro-scale sensors that can detect electrical surface property changes, a capability of APM devices, due to their bare sensing surfaces. Excitation occurs through electrodes that usually conform to the substrate as half-moon [Fig. 2(a)] or bite-wing variants [5]. As larger devices, the electrode patterning and deposition processes are relatively simple, and the smallest dimension – the electrode gap – is usually on the order of a millimeter in size. Precise excitation can be achieved without deposited electrodes [11], allowing observation of the impact of the lateral electric field direction without mechanical electrode loading. Polishing the surfaces for low surface roughness and slowly varying curvatures [Fig. 2(b)] is also possible.

As LFE electrodes do not strongly support lateral wavelengths like IDTs, the extended Christoffel-Bechmann (CB) elastic wave formalism [12] predicts thickness mode excitation. For AT-cut quartz, the quasi fast shear and quasi extensional/longitudinal thickness modes are excited by an x_1 oriented electric field. The pure slow TSM is excited by an x_2 oriented electric field, aligned with the crystal flat [Fig. 2(a)]. Though both LFE and TFE can excite the pure slow TSM, LFE-QCMs are far weaker in response than theorized and when compared to standard QCMs. The reason for these weak responses is that LFE modes are comprised of APWs. Were an ideal 0-diopter (plano-plano) QCM laterally infinite, only the pure TSM would exist. For LFE, the APWs would propagate indefinitely and never resonate. The finite extent and 10 µm surface roughness average of 0-diopter samples allow weak and spurious resonances, as shown in Fig. 3. This reasoning is supported by the improvement from plano-convex samples

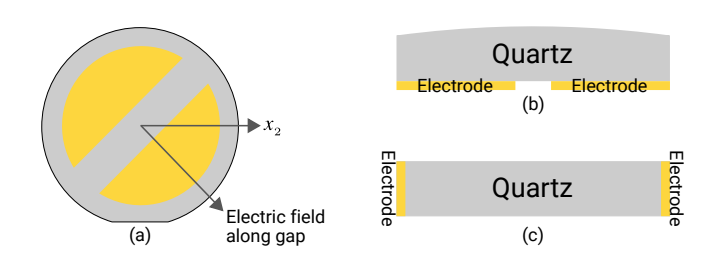


Fig. 2. (a) LFE-QCM with half-moon electrodes and alignment flat, (b) planoconvex LFE-QCM, and (c) idealized plano-plano LFE-QCM.

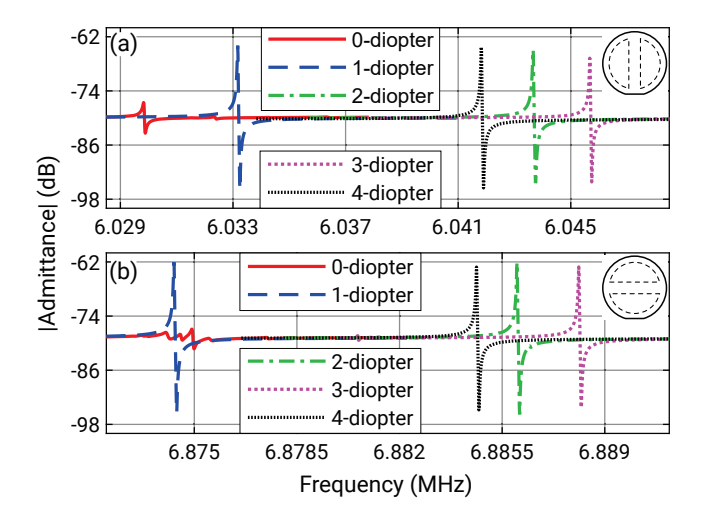


Fig. 3. Corresponding LFE-QCM configurations with (a) pure slow and (b) quasi fast TSM admittance magnitude responses for varying diopter.

with curvature as slight as a single diopter for both TSMs, which persists for higher curvatures.

The formulation assumptions for the CB formalism do not account for the APWs in LFE devices. The thickness mode excitation relies on a constant lateral electric field applied through electrodes on the lateral surfaces [Fig. 2(c)]. Furthermore, only thickness variation of solutions is considered. For the electrically open boundaries and throughout the substrate, the normal electric displacement is assumed to be zero [13]. This approximation qualitatively predicts mode excitation for various materials, as the normal electric displacement vanishing at electrically open surfaces is not rare for APWs [9]. However, thickness analysis does not allow the nonzero electric potential - present for LFE-QCMs - to vanish at infinity. For plane wave solutions, there must then be a nonzero β and thus laterally propagating wave solutions overall. The main LFE mode is then an APM, and the CB formalism retains consistency for small β .

The superposition of partial waves method [1] is a more appropriate analysis for LFE devices with varying boundary conditions. The electric field orientation is then the direction of propagation, just as for TFE. Mode excitation is indicated by the changes in wave characteristics from electrical boundary conditions [14]–[16]. The two-dimensional APW analysis is consistent with the LFE wave components of AT-cut quartz. For propagation along x_1 , only stiffened SH waves occur. For propagation along x_1 , all displacements are coupled to the potential. From the CB formalism, $qSH_1^{(1)}$ (branch with quasi fast shear cutoff) and $qS_1^{(1)}$ (branch with quasi extensional cutoff) modes with small β are excited.

A. Impact of a Thin Conducting Film

For the conducting film data, the samples had 6 MHz pure slow TSM series resonance frequency, 13.97 mm diameter, 6.35 mm diameter deposited metal films, and no deposited electrodes. A printed circuit board (PCB) [11] with 9 mm

diameter half-moon electrodes and a 0.5 mm electrode gap was used for excitation. Varying the lateral electric field direction excited two dominant modes, the 0° and 90° modes [11], based on the angle between the electrode gap and the flat. With a 10 nm thick Cr film, the 0-diopter 0° and 90° modes remained near the pure slow TSM frequency, and the response intensity improved [Fig. 4(a)]. For minimal spurious mode presence, a 2-diopter sample with a 20 nm thick Cr film was used to observe the main mode response variation with electric field rotation, as shown in Fig. 4(b). The 0° and 90° modes were both present with somewhat lower intensities and electromechanical couplings (separations between series and parallel resonance frequencies) at 45°. Like the increase in frequency for 0- to 2-diopter, the metal-loaded LFE-OCM resonance frequencies strictly rose for 0- to 4-diopter, indicating consistently larger trapped β from greater curvature.

Increasing the Cr film thickness increased the film conductance toward an electrical short, and the mode response increased. The metal-loaded modes were also observed to arise for an Au film thickness as low as 5 nm. However, the modes were relatively weak because of the low film conductance. The modes transitioned back to the usual air-loaded LFE modes when the Au film was made effectively discontinuous through a heat treatment below the Curie temperature of quartz. The electrically open Au film was verified through an optical microscope, multimeter, and four-point probe.

The metal film thickness results indicate the need for sufficient lateral film conductance for mode interaction. Increased mode response and differing excited modes are common for varying electrical boundary conditions on APM devices [15]. The higher metal-loaded 0-diopter LFE-QCM frequencies are likely due to the β trapped by the finite metal film. Given the proximity of the metal-loaded modes to the slow pure TSM in the 0-diopter samples, the 0° mode is an $SH_1^{(2)}$ mode, while the 90° mode is a $qA_1^{(1)}$ mode. Both these APMs have the pure

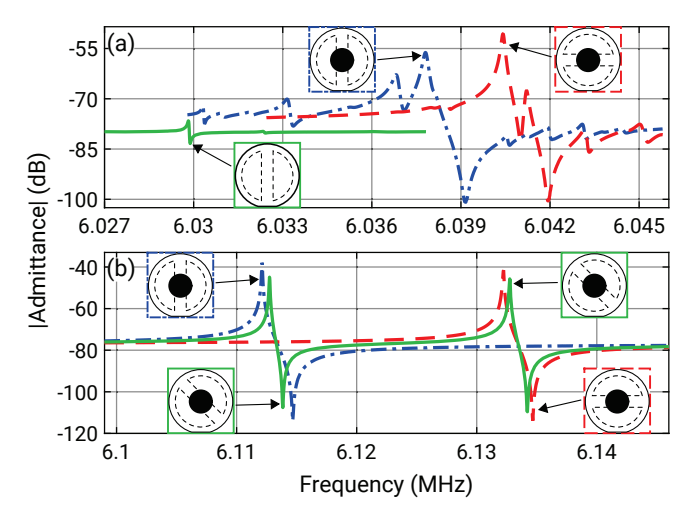


Fig. 4. Corresponding LFE-QCM configurations with (a) 0-diopter LFE-QCM mode response comparison for air-loaded vs. metal-loaded, (b) mode variation for 2-diopter metal-loaded LFE-QCM for electric field rotation.

slow TSM as their cutoff and deviate slightly in frequency for small β . There were lesser resonances roughly 100 kHz away from the main modes that were likely other APMs.

B. Impact of a Thin Semiconducting Film

For the semiconducting film data, the samples had 6 MHz pure slow TSM resonance frequency, 13.97 mm diameter, 3-diopter surface curvature, deposited WO₃ films, and no deposited electrodes. The PCB with 9 mm diameter halfmoon electrodes and a 0.5 mm electrode gap was used for excitation. The films were 0, 50, and 100 nm thick with 6.35 mm diameters. The film conductivity varied by altering the quantity of film oxygen vacancies through the Ar/O₂ ratio used during reactive sputtering of the tungsten. The ratios were 20/80, 50/50, and 80/20. In Fig. 5, for the 20/80 and 50/50 ratios, the pure slow TSM responses were present within the expected range of response intensities for all film thicknesses. However, the 80/20 films attenuated the modes at both 50 and 100 nm thicknesses. The mode attenuation increased with film thickness, and all the modes were no longer present for 100 nm, even with electric field rotation. The greatest conductivity occurred in the 80/20 film due to the least O2 used, with the greatest conductance at 100 nm thick. Attenuation from media with moderate conductivities like semiconductors and liquids is expected for APMs [9], [17].

IV. CONCLUSIONS

The purpose of this work was to clarify that LFE-QCMs operate through APMs. All of the results for LFE-QCMs are explainable from the perspective of APM devices. Plate wave analysis is consistent with the usual LFE theory for AT-cut quartz and is more appropriate for real LFE-QCMs with varying electrical boundary conditions. Based on the reported metal-loaded LFE-QCM results, it is inferred that the metallization strongly excites $SH_1^{(2)}$ and $qA_1^{(1)}$ modes for the present β . Semiconducting film results are also consistent with

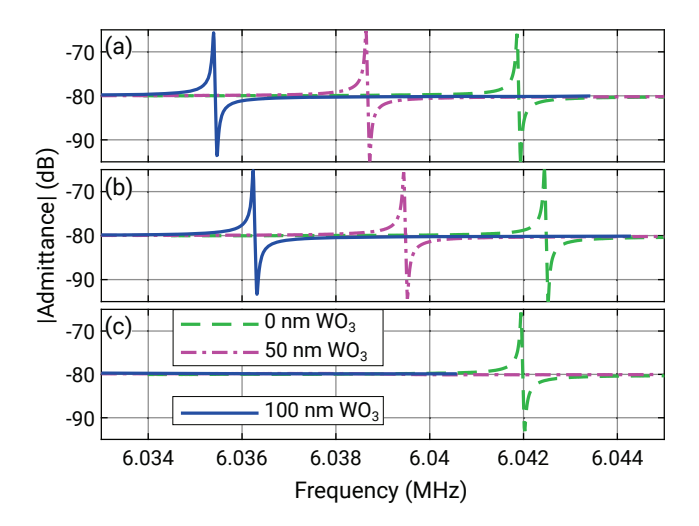


Fig. 5. Impact of semiconducting films on LFE-QCM pure slow TSM mode responses: (a) 20/80, (b) 50/50, and (c) 80/20 Ar/O₂ ratios.

known APM results. As the active dispersion branch and mode electromechanical coupling may change, it is not sufficient to analyze only frequency shifts when sensing electrical properties with LFE devices. Given this work, it is hoped that LFE sensor research may be enriched by results and insight arising from all areas of APM device research.

ACKNOWLEDGMENT

This work has been supported by the National Science Foundation (NSF) grants 1851998 "REU Site: Sensor Science and Engineering" and 1701087 "PFI:AIR - TT: Lateral Field Excited Acoustic Wave Sensor for Monitoring Thin Film Properties in Solid State Devices." The high-quality AT-cut quartz blanks were obtained from Fil-Tech, Inc. Jackson Hall, an NSF-REU student, produced the LFE-QCMs with deposited semiconducting films and acquired the response data.

REFERENCES

- B. A. Auld, Acoustic Fields and Waves in Solids. New York: Wiley, 1974, vol. 2.
- [2] H. Bhugra and G. Piazza, Eds., Piezoelectric MEMS Resonators. Cham, Switzerland: Springer, 2017.
- [3] J. F. Rosenbaum, Bulk Acoustic Wave Theory and Devices. Norwood, MA: Artech House, Inc., 1988.
- [4] V. Plessky, S. Yandrapalli, P. J. Turner, L. G. Villanueva, J. Koskela, and R. B. Hammond, "5 GHz laterally-excited bulk-wave resonators (XBARs) based on thin platelets of lithium niobate," *Electron. Lett.*, vol. 55, no. 2, pp. 98–100, 2019.
- [5] J. S. R. Hartz, N. W. Emanetoglu, C. Howell, and J. F. Vetelino, "Lateral field excited quartz crystal microbalances for biosensing applications," *Biointerphases*, vol. 15, no. 3, p. 030801, 2020.
- [6] Y. Jin and S. G. Joshi, "Propagation of a Quasi-Shear Horizontal Acoustic Wave in Z-X Lithium Niobate Plates," *IEEE Trans. Ultrason. Ferroelectr. Freq. Control*, vol. 43, no. 3, pp. 491–494, 1996.
- [7] E. L. Adler, "Electromechanical Coupling to Lamb and Shear-Horizontal Modes in Piezoelectric Plates," *IEEE Trans. Ultrason. Ferroelectr. Freq. Control*, vol. 36, no. 2, pp. 223–230, 1989.
- [8] T. M. Niemczyk, S. J. Martin, G. C. Frye, and A. J. Ricco, "Acoustoelectric interaction of plate modes with solutions," *J. Appl. Phys.*, vol. 64, no. 10, pp. 5002–5008, 1988.
- [9] F. Zhu, B. Wang, Z. Qian, I. Kuznetsova, and T. Ma, "Influence of Surface Conductivity on Dispersion Curves, Mode Shapes, Stress, and Potential for Lamb Waves Propagating in Piezoelectric Plate," *IEEE Trans. Ultrason. Ferroelectr. Freq. Control*, vol. 67, no. 4, pp. 855–862, 2020.
- [10] J. Yang, Vibration of Piezoelectric Crystal Plates. Singapore: World Scientific Publishing Co. Pte. Ltd, 2013.
- [11] J. S. R. Hartz, J. F. Vetelino, and N. W. Emanetoglu, "Investigation of Energy Trapping of the Lateral Field Excited Thickness Shear Mode in AT-Cut Quartz Crystal Microbalances," in *IEEE Int. Ultrason. Symp.*, Glasgow, United Kingdom, 2019, pp. 596–599.
- [12] A. Ballato, "Extended Christoffel-Bechmann Elastic Wave Formalism for Piezoelectric, Dielectric Media," in *Proc. IEEE/EIA Int. Freq. Control Symp. Exhib.*, 2000, pp. 340–344.
- [13] T. Yamada and N. Niizeki, "Formulation of Admittance for Parallel Field Excitation of Piezoelectric Plates," *J. Appl. Phys.*, vol. 41, no. 9, pp. 3604–3609, 1970.
- [14] K. Toda and K. Mizutani, "Propagation Characteristics of Plate Waves in a Z-Cut X-Propagation LiTaO₃ Thin Plate," *Electron. Commun. Japan*, vol. 3, no. 8, pp. 1225–1233, 1989.
- [15] C.-M. Lin, V. Yantchev, Y.-Y. Chen, V. V. Felmetsger, and A. P. Pisano, "Characteristics of AlN Lamb Wave Resonators with Various Bottom Electrode Configurations," in *Jt. Conf. IEEE Int. Freq. Control Eur. Freq. Time Forum*, San Francisco, CA, 2011, pp. 505–509.
- [16] J. Zou, C.-M. Lin, and C. S. Lam, "Transducer design for AlN Lamb wave resonators," J. Appl. Phys., vol. 121, no. 15, 2017.
- [17] B. D. Zaitsev, I. E. Kuznetsova, S. G. Joshi, and I. A. Borodina, "Acoustic waves in piezoelectric plates bordered with viscous and conductive liquid," *Ultrasonics*, vol. 39, no. 1, pp. 45–50, 2001.